Journal of *Marine Science and Engineering*

MDPI

Article

Probability of Atlantic Salmon Post-Smolts Encountering a Tidal Turbine Installation in Minas Passage, Bay of Fundy

Brian G. Sanderson [1,*], Richard H. Karsten [2], Cameron C. Solda [3], David C. Hardie [4] and Daniel J. Hasselman [5,*]

1 Acadia Centre for Estuarine Research, Acadia University, Wolfville, NS B4P 2R6, Canada
2 Department of Mathematics and Statistics, Acadia University, Wolfville, NS B4P 2R6, Canada; richard.karsten@acadiau.ca
3 Department of Biology, Acadia University, Wolfville, NS B4P 2R6, Canada; cameronsolda@acadiau.ca
4 Department of Fisheries and Ocean, Dartmouth, NS B2Y 4A2, Canada; david.hardie@dfo-mpo.gc.ca
5 Fundy Ocean Research Center for Energy, Halifax, NS B3J 3N5, Canada
* Correspondence: bxs@bellaliant.net (B.G.S.); dan.hasselman@fundyforce.ca (D.J.H.); Tel.: +1-902-697-2592 (B.G.S.); +1-902-406-1166 (ext. 7) (D.J.H.)

Abstract: Tidal stream energy is a renewable energy resource that might be developed to offset carbon emissions. A tidal energy demonstration (TED) area has been designated in Minas Passage, Bay of Fundy, for testing and installing marine hydrokinetic (MHK) turbines. Regulations require quantification of the potential for MHK turbine installations to harm local populations of marine animals. Here, we use acoustic telemetry to quantify the probability that post-smolt inner Bay of Fundy salmon encounter a turbine installation at the TED area. Previous work has quantified the detection efficiency of Innovasea HR acoustic tags as a function of the current speed and range from a moored HR2 receiver and also demonstrated that drifters carrying HR tags will be effectively detected when the drifter track crosses the array of HR2 receivers in Minas Passage. Salmon smolts were tagged and released in Gaspereau and Stewiacke Rivers, Nova Scotia, in order that the HR2 receiver array could monitor seaward migration of the post-smolts through Minas Passage and particularly through the TED area. Presently, we formulate and apply a method by which tag signals detected by the HR2 array can be used to estimate the expected number of times that a post-smolt would encounter a single near-surface MHK turbine installation during its seaward migration.

Keywords: fish; MHK turbine; probability of encounter; tidal energy; Atlantic salmon; smolt; acoustic telemetry

Citation: Sanderson, B.G.; Karsten, R.H.; Solda, C.C.; Hardie, D.C.; Hasselman, D.J. Probability of Atlantic Salmon Post-Smolts Encountering a Tidal Turbine Installation in Minas Passage, Bay of Fundy. *J. Mar. Sci. Eng.* **2023**, *11*, 1095. https://doi.org/10.3390/jmse11051095

Academic Editor: Jose Pedro Andrade

Received: 21 April 2023
Revised: 15 May 2023
Accepted: 17 May 2023
Published: 22 May 2023

1. Introduction

A large human population that depends on energy-dense fossil fuels [1] causes environmental changes [2]. Large amounts of renewable energy might be harvested from the tides of Canada's Bay of Fundy [3] to offset the use of fossil fuels. It is hoped that ecosystem disruption can be reduced by obtaining energy from renewable resources. Historically, however, exploitation of renewable energy has not been ecologically benign. In Europe, the spread of watermill technology from the early Middle Ages to early modern times has been associated with the dramatic decline of Atlantic salmon (*Salmo salar*) populations [4]. More recently, measurements showed 39% mortality for 0.136 m juvenile striped bass (*Morone saxatilis*) immediately after passing through a low-head turbine [5]. On the other hand, very little mortality was observed for a low-head turbine that was specially designed for fish safety [6]. At Anapolis Royal, Bay of Fundy, fish mortality has been associated with the 20 MW reaction turbine that relied upon a tidal barrage to create a pressure head [7].

Marine hydrokinetic (MHK) turbines harvest kinetic energy of ocean currents rather than relying on a pressure head. Without a pressure head, a turbine must have a larger diameter to produce the same amount of power, but fish-damaging pressure forces (and shear stress) may be reduced, depending upon turbine design. A tidal barrage directs

much of the flow through a turbine, whereas MHK turbines often obstruct only a small proportion of the tidal flow and a flood or ebb tide might see many fish pass by without encountering a turbine.

A 1.6 km × 1 km tidal energy demonstration (TED) area has been designated for deploying MHK turbines in Minas Passage where the current can exceed 5 m s^{-1} [8,9]. Three gravity-base MHK turbines (up to 2 MW) have been tested at the TED area, but their interactions with fish remain unquantified. Given that Minas Passage is approximately 5 km wide, it is fair to say that most fish would not encounter a turbine during an ebb or flood tide. Quasi-stable drifter tracks pass repeatedly back and forth through Minas Passage but most of those tracks pass to the south of the TED area and, therefore, have low probability of encountering a MHK turbine installation [10]. Other drifter tracks through the TED area have been observed to subsequently disperse elsewhere [9,10], which indicates that, should an individual fish encounter a MHK turbine, then that experience would not be repeated for many of the following tidal cycles.

Quantifying whatever harm a MHK turbine may or may not do to a fish population begins with the probability of an individual encountering the turbine. A definition for probability of a fish encountering a MHK turbine is a precondition for unambiguous calculation from practicable measurements.

Definition 1. *Probability of encounter is the probability that—at some location, during some time interval* $t_0 \leq t \leq t_0 + T$*—a fish that belongs to a distinguishable population will pass through the area* A_{MHK} *that would be swept by the blades of a MHK turbine without the turbine actually being deployed at that position at that time.*

The probability of encounter can only be considered to be an upper limit on the probability of harm. If a MHK turbine is present, then there is always a possibility that an individual will simply avoid swimming through A_{MHK}. An idealized turbine operating at the Betz limit [11] diverts about 30% of the incoming flow around A_{MHK}, so an individual might sometimes avoid the turbine by passively drifting with the flow. In clear tropical waters with comparatively weak currents, video observations showed large fish avoiding a small MHK turbine, whereas smaller fish sometimes passed through the turbine but evaded the blades [12]. At higher latitude, video footage showed fish aggregating near a MHK turbine at slack-water high-tide [13] but that analysis subsampled observations to an extent that neither fish-turbine encounter nor avoidance behaviour could be estimated when the tidal current was faster. Studies in an open channel flume showed both avoidance behaviour and salmon evading turbine blades [14]. Echosounder transects [15,16] and analysis of images taken by acoustic cameras [17] both indicated avoidance behaviour by fish upstream from a MHK turbine in ≈2 m s^{-1} tidal currents at Cobscook Bay. At a high latitude MHK turbine site, echosounder measurements showed fish aggregation near slack water and an indication of avoidance behaviour when the tidal current was faster [18]. Such measurements of avoidance and blade evasion have not been successfully achieved in the more challenging conditions at Minas Passage [19].

Previous measurements and analysis [10] indicate that fast tidal currents dominate fish movement in Minas Passage, so given the abundance (number of individuals per unit horizontal area) and distribution of a population of interest, then it is straightforward to estimate the probability of an encounter from the tidal flux through A_{MHK}. In practice, abundance has not been accurately quantified for any population found in Minas Passage [17,19]. Nevertheless, the following work will show how the probability of encounter can be estimated from a different method which uses acoustic telemetry to detect acoustically tagged individuals as they pass by acoustic receivers in the TED area.

Early efforts implanted Innovasea 69 kHz pulse position modulation (PPM) tags in the body cavities of striped bass belonging to a local population that spawns in the Shubenacadie River, Nova Scotia [20]. Similarly, 69 kHz PPM tags were implanted in Atlantic sturgeon (*Acipenser oxyrhinchus*) that were mostly from the Saint John River, New Brunswick,

population stock [21]. While these measurements were useful for demonstrating swimming depth and presence near the TED area [20–22], range detection measurements [23] indicated that presence would often be undetected when the tidal current was fast. Undetected presence was unambiguously demonstrated when an array of receivers in the TED area often failed to detect a passing drifter that carried a 69 kHz PPM tag when currents were fast and yet many receivers in the array concurrently detected the tag signals when currents were slow [9]. Drifters also carried 170 kHz High Residency (HR) tags that did enable passing drift tracks to be reliably detected in fast tidal currents [9]. In 2019, post-spawn alewives (*Alosa pseudoharengus*) in Gaspereau River, Nova Scotia, were implanted with HR tags and were detected during their seaward migration through Minas Passage [24].

Three gravity-base MHK turbines have been installed at the TED area but now only one remains and it is in a non-operational state. MHK turbines may also be installed on floating platforms [25,26]. Such near surface turbines raise concerns for the safety of Atlantic salmon because they swim near the sea surface [27,28]. Canada's *Species At Risk Act (SARA)* lists inner Bay of Fundy Atlantic salmon as endangered and the Department of Fisheries and Oceans (DFO) operates a hatchery stocking program [29] that presently makes a significant contribution to the population by releasing unfed fry at freshwater locations that provide suitable habitat.

In the following work, we estimate the probability that individual post-smolts would encounter MHK turbines at the TED area in Minas Passage. Specifically, HR acoustic tags were implanted within the body cavities of smolts as they migrated down river and an array of HR2 receivers was installed to detect them as they passed through Minas Passage. By considering a moored HR2 receiver as a proxy for some yet-to-be installed MHK turbines and utilizing results from our studies of detection efficiency [9,30], it is possible to estimate the probability of a fish–turbine encounter when a tagged post-smolt is detected passing through the TED area.

2. Materials and Methods

As an outline, the method is to deploy an array of moored HR2 receivers within and nearby the TED area in order to detect post-smolts that were tagged earlier during their seaward migrations from Gaspereau River and the Stewiacke River (Figure 1). Previous work has quantified the detection efficiency of HR2 receivers that were deployed within the TED area in 2021 [30]. Here, we detect tagged post-smolts as they pass by receivers and develop a method to convert that information into a probability of an encounter at and near the TED area.

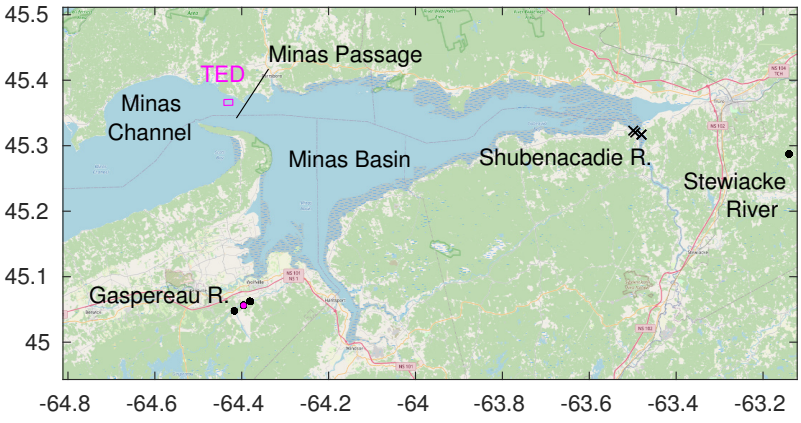

Figure 1. Locations in Minas Passage and neighbouring waters. Black dots show where 2019 smolts were released in Gaspereau River and Stewiacke River. Stewiacke River is a tributary to Shubenacadie River which connects to Minas Basin. Magenta dot shows release site for smolts tagged in 2022. Black crosses show positions of VR2W-180 kHz receivers moored near the mouth of Shubenacadie River.

2.1. Receiver Arrays

In 2019, the Fundy Ocean Research Centre for Energy (FORCE) moored four HR2 receivers in Minas Passage at positions marked S2, W1, W2, and D1 (Figure 2). Each mooring used SUBS-Model A2 (Open Seas Instrumentation Inc., Musquodoboit Harbour, Canada) with an acoustic release that was tethered to a 240 kg steel weight by a 3 m riser. Innovasea HR2 and VR2W-69 kHz receivers were attached just forward of the tail fin of each SUBS. The volcanic plateau within the TED area is favoured for MHK turbines and only the D1 mooring was deployed at that site but moorings W1 and W2 are also judged as useful because they are aligned with the tidal flow over the volcanic plateau. Mooring S2 provides a comparison for locations nearer the middle of Minas Passage. The FORCE moorings are primary to the present study but peripheral use will be made of Innovasea receivers that were deployed by other organizations (Ocean Tracking Network, Acadia University, Department of Fisheries and Oceans) at other locations in Minas Passage, Minas Basin, and the Gaspereau River [24].

In 2022, FORCE deployed 11 SUBS at mooring sites (Figure 2) that were generally aligned orthogonal to the tidal current with most positions selected to place receivers on local high ground where the available high-resolution bathymetry indicated relatively low local variation. Again, a SUBS-Model A2 was used with an acoustic release and a 3 m riser from a 240 kg weight. In 2022, the HR2 receiver was housed mostly within the SUBS with its hydrophone sensor protruding above the hull of the SUBS and the VR2W-69kHz receiver was mounted directly behind the tail fin. The 2022 receiver array has previously been used for further range testing and for confirming that receivers will detect tags carried beneath drifters that pass over the array [9]. HR2 receivers at sites 9 to 12 monitor trajectories over that part of the volcanic plateau where MHK turbines are most likely to be deployed in the future, whereas sites 1, 2, and 4 to 8 enable comparison to the south. Mooring 3 failed [9].

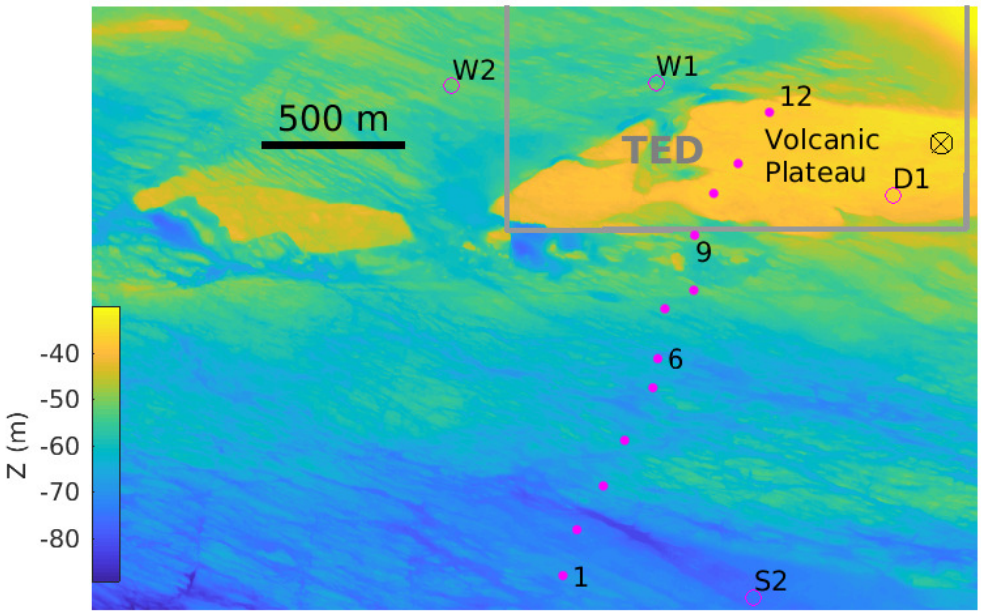

Figure 2. Mooring locations in Minas Passage. HR2 receivers were moored at sites S2, W1, W2, and D1 (magenta circles) in 2019. HR2 receivers were moored at sites 1−2 and 4−12 in 2022 (magenta dots).

2.2. Tagging Smolts

Tagging conducted during 2019 was registered under DFO Scientific License to Fish license # 330657 and salmon surgical procedures were performed under Acadia University Animal Care Committee protocol #07-18.

Smolts were captured during their down-river migration. Innovasea V5 HR tags were surgically implanted and after a recovery period the smolts were released to continue their

migration. Tags were programmed to transmit a 170 kHz, 143 dB high residency (HR) signal every 1.8 s to 2.2 s and a 180 kHz pulse position modulation (PPM) signal every 25 s to 35 s.

From 7 to 18 May 2019, 87 smolts from the Gaspereau River were captured and tagged near the bypass dam (Figure 1, [24]) where the DFO hatchery program has a fish trap. Tagged smolts were released upstream of the bypass dam, in the pool at the foot of the bypass dam, and 2 km further downstream in the Gaspereau River. From 20 May to 12 June 2019, 57 smolts were captured, tagged and released in the Stewiacke River (Figure 1).

In 2022, smolt capture was conducted under a scientific sampling permit issued to D Hardie and surgical procedures were approved under the Acadia University Animal Care Committee protocol #08-22. Smolts were captured in the DFO trap at the bypass dam during their migration down the Gaspereau River. There were 25 smolts tagged and they were all released into the pool below the bypass dam. Tagging and releases were performed in three groups: 9 smolts on 9 May, 8 on 10 May, and 8 on 11 May.

2.3. Detection Efficiency and Tidal Current

Definition 2. *Detection efficiency ρ is the probability that a signal transmitted by a tag will be detected by a nearby receiver.*

Measurements of detection efficiency have been made at the TED site in Minas Passage for both HR signals and 180 kHz PPM signals [9,30]. Detection efficiency declines with increasing range from transmitting tag to receiver and also declines with increased tidal current speed. The HR signals are more efficiently detected than PPM signals and also have the advantage of being able to be transmitted more frequently. Frequent transmission is of paramount importance for detecting a tagged fish as it passes by because even in fast currents there will be brief intervals when ambient noise levels are lower than typical and a signal can be detected [9]. Detection efficiency can be related to the area that is effectively monitored [30] and will similarly play a central role in the following calculation of probability of fish–turbine encounters.

2.4. Tidal Current

The detection efficiency $\rho(r, s)$ has been measured as a function of range r from tag to receiver and vertically averaged flood/ebb tidal current speed s at the site of the HR2 receiver [30]. Tidal current speed is designated s positive on the flood tide and negative on the ebb. It was not usually possible for us to directly measure tidal current speed so values of s were downloaded from a FVCOM simulation [3,8,31].

The FVCOM current speed s is always used for the calculation of detection efficiency because ρ was empirically parameterized as a function of s [30]. For some other purposes it will be more appropriate to use drifter speed s_d, which [9] has empirically related to s

$$s_d = \begin{cases} (s - 0.14)/0.87 & \text{Within the TED area} \\ (s - 0.07)/0.76 & \text{South of the TED area.} \end{cases} \quad (1)$$

2.5. Detecting Passing Events

Small fish, such as post-smolts and alewife, are substantially moved past moored receivers by the fast tidal currents in Minas Passage [10,24]. A passing event is presently understood to be the time when a sequence of closely spaced HR signals are detected from a tagged post-smolt that is passing a line of receivers. The relationship between detection efficiency ρ and detection of a passing event has been quantified in detail using tags that are carried by GPS-tracked drifters [9]. Sometimes the same passing event was recorded by more than one mooring and in such instances we consider the smolt to have passed by the mooring station that detected the most signals. Thus, for a flood tide (or an ebb tide) there can be at most one passing event for any particular post-smolt and this preserves the statistical independence of all passing events.

To estimate the probability of encounter, we consider that the receiver that detects the passing event is replaced by a hypothetical turbine that has the same x, y coordinates but with a z coordinate representative of the type of turbine that is of interest. The Lagrangian coordinate applies most naturally to the trajectory of a post-smolt, as it would for most moving animals. There are two Lagrangian methods that might be used to convert a set of passing events to an estimate of probability of encounter.

1. Measure the distance of closest approach of each passing tagged fish to the receiver (proxy turbine) and identify those that were close enough to cross the area A_{MHK} that would be swept by turbine blades. Two measurement methods might be used.
   (a) The number of signals that are detected during a passing event will typically be larger if the smolt passes closer to the receiver. Drifter studies demonstrate much variability in the measured number of detections relative to the expected number [9].
   (b) Use many closely spaced HR2 receivers to localize the track of each tagged fish as it passes by. Measurements of detection efficiency [30] indicated an impractical number of receivers would be required.
2. Another approach is to consider that a detected passing event might have been on any one of a set of all paths that passed the receiver/turbine. This approach builds on an assumption of statistical similarity for paths that cross within a scale comparable to the effective range of detection [9]. This was the approach that was previously used to calculate the probability that drifters would collide with a turbine installation in Minas Passage [10]. Presently, we build upon this approach.

2.6. Calculation of Probability of Encounter

The measured detection efficiency for a HR signal ρ is a function of range r and current speed s [9]. Here, $r = \sqrt{x^2 + y^2 + z^2}$ is the slant range from a near-surface tagged post smolt to a HR2 receiver at the origin of the horizontal plane $x = 0, y = 0$ but at depth z relative to the post-smolt. Without loss of generality, we consider a coordinate system so that the ensemble of possible post-smolt trajectories travel in the x-direction so that their y coordinate becomes the horizontal distance of the closest approach of the tagged post-smolt to the moored HR2 receiver that detected the passing event. Figure 3 lays out the situation with two mathematically convenient symmetries. The first symmetry is that $r(x, y, z) = r(x, -y, z)$, so we only need to perform the calculation on the positive y half-plane. The second symmetry is that ρ will be the same for a tag on the smolt and receiver at the origin as for a receiver on the smolt and a tag at the origin.

Consider an encounter with one side of a turbine installation that has total width W oriented across-current and centered on the origin in Figure 3. A presently planned turbine installation consists of six near-surface turbines that have been estimated to span an effective width of $W = 38$ m [10,25,26]. Post smolts swim near the sea surface [28], so to a first approximation we consider that they are within the depth range spanned by the blades of the turbines. To the extent that this approximation does not apply for some specific turbine installation, a correction factor can be estimated and applied after the following.

Consider a tagged smolt at position x, y, z relative to the HR2 receiver that detects a passing event. The HR2 receiver can be considered to be a proxy for a turbine installation at the same position except for the HR2 being a distance z below both the turbine installation and the post-smolt that might encounter it. Thus, the range from post-smolt to HR2 is $r = \sqrt{x^2 + y^2 + z^2}$ and we write $\rho(r, s) = \rho(x, y|z, s)$ to represent the detection efficiency along tracks that share the same values for z and s. Figure 3 uses color to show detection efficiency on the half-plane.

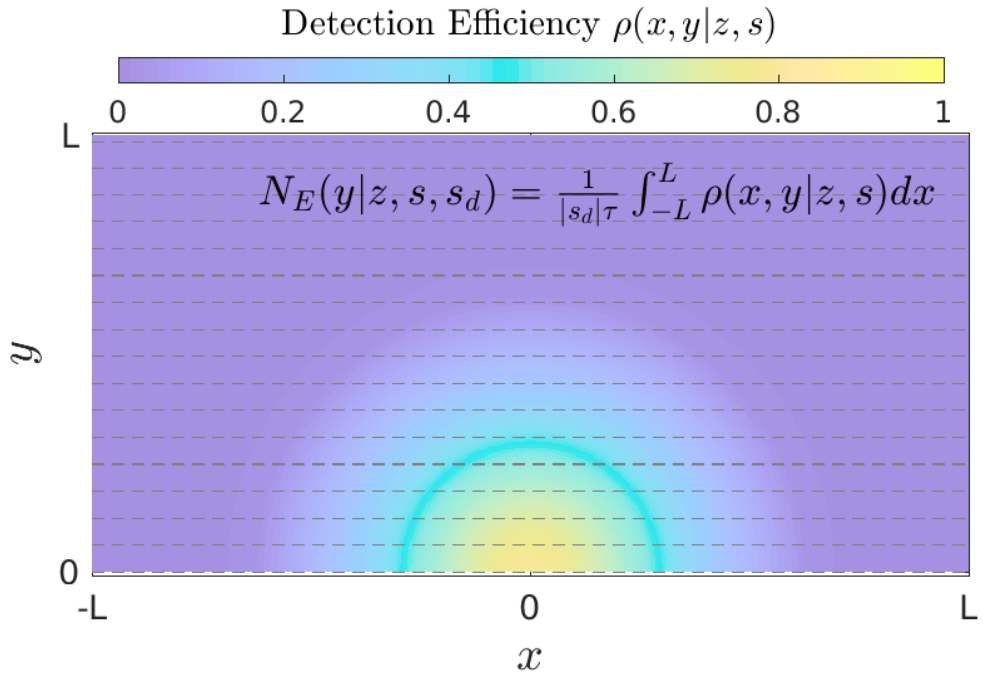

Figure 3. Plan view of an ensemble of smolt tracks (dotted lines in the $x-$direction) that pass within a distance y of a receiver/turbine that is located at the origin. The color scale shows probability of detecting a transmitted signal depending upon the position of a smolt.

Tracks with larger y are less likely to be detected. Following [9], the number of signals expected to be detected along the length of a track is

$$N_E(y|z, s, s_d) = \frac{1}{|s_d|\tau} \int_{-L}^{L} \rho(x, y|z, s)dx \tag{2}$$

where τ is the time scale between signals transmitted by the tag and $L = 350$ m is the range beyond which ρ is effectively zero. The calculation of travel distance $|s_d|\tau$ between HR signals uses drift speed s_d (1). Equation (2) identifies the expected number of times that a tag would be detected if it passed by an HR2 receiver along a track with closest approach y. N_E is a real number≥ 0. The expected probability that at least one signal will be detected along that track with closest approach y is

$$p_E(y, |z, s, s_d) = \min(N_E(y|z, s, s_d), 1). \tag{3}$$

Tracks passing close to the turbine (small y) would have $N_E \gg 1$ and, therefore, $p_E = 1$, because at least one signal would be detected. Tracks passing further away from the turbine (larger y) have $1 > N_E \geq 0$ and $p_E = N_E$ (i.e., the expected number of detected signals is the probability of detecting a signal). Given (3), the expected probability of encounter would be

$${}^{E}\mathcal{P}(z, s) = \frac{\int_0^{W/2} p_E(y|z, s)dy}{\int_0^{L} p_E(y|z, s)dy} \tag{4}$$

where we note that ${}^{E}\lambda = \int_0^{L} p_E(y|z, s)dy$ can be considered to be half the cross-current width over which passing tags are expected to be detected.

Experiments using tags suspended beneath GPS-tracked drifters compared measured values for the number of detected signals N_D (integers≥ 0) against the expected number N_E (real numbers≥ 0) (see Figure 7 of [9]) and a linear regression gave

$$\sqrt{N_D} = -0.30 + 0.87\sqrt{N_E} \tag{5}$$

Given (5) and the physical requirement that the number of signals must be ≥ 0, it seems that an improved estimate for the expected number of signals detected along a track would be

$$\mathcal{N}(y|z,s,s_d) = \left[\max\left(-0.30 + 0.87\sqrt{N_E}, 0\right)\right]^2 \quad (6)$$

and the probability of the track with closest approach y being detected would be

$$p(y,|z,s,s_d) = \min(\mathcal{N}(y|z,s,s_d), 1) \quad (7)$$

in which case a better estimate of the probability of encounter $\mathcal{P}$ might be calculated as the ratio of two cross current scales,

$$\mathcal{P}(z,s,s_d) = \frac{\int_0^{W/2} p(y|z,s,s_d)dy}{\lambda} \quad (8)$$

$$\lambda(z,s,s_d) = \int_0^{L} p(y|z,s,s_d)dy, \quad (9)$$

the numerator of (8) being the effective half-width of the turbine installation and the denominator, λ, being the effective half-width of all passing tracks that might be detected.

$\mathcal{P}$ is backed by the more thorough set of measurements, relying on both empirical estimation of ρ and empirical testing of how ρ relates to detecting tags carried by GPS-tracked drifters as they pass by a receiver with a measured distance of closest approach. ${}^{E}\mathcal{P}$ is only backed by Eulerian measurements of ρ but is easier to obtain from an experimental point of view. It will be of interest to compare ${}^{E}\mathcal{P}$ with $\mathcal{P}$ in view of the possibility of improving results by obtaining more drifter measurements in future.

3. Results

In 2022, the FORCE array spanned much more of the width of Minas Passage than did the 2019 FORCE array (Figure 2). It is, therefore, expected that in 2019 a tagged post-smolt was less likely to be detected during its migration through Minas Passage than in 2022. On the other hand, more smolts were tagged in 2019.

3.1. Presence of Tagged Post-Smolts in Minas Passage

In 2022, there were 11 HR2 receivers in the FORCE array at Minas Passage (Figure 2) and they detected 22 of the 25 smolts that were tagged in Gaspereau River. One additional post-smolt was detected by the Ocean Tracking Network (OTN) array that is also in Minas Passage and less than 2 km east of the FORCE array. The OTN array is only relevant to the present objective in so much as it confirms that at least 23 tagged post-smolts arrived at Minas Passage. The same two post-smolts that were not detected in Minas Passage were also the only smolts not detected by receivers in the tidal section of Gaspereau River. Receivers between the release location and tidal Gaspereau detected 24 tagged smolts. Applying the appropriate analysis—Equation (3) of [24]—the most probable estimate is that $N_{\mathrm{MP}} = 23$ tagged post-smolts migrated into Minas Basin and they all reached Minas Passage. There was no apparent mortality for that part of the migration from the mouth of Gaspereau River to Minas Passage [27].

In 2019, the FORCE array had only four HR2 receivers that spanned a small portion of the Minas Passage cross-section (Figure 2) [24]. Those receivers detected 43 of the 87 smolts tagged in Gaspereau River and 29 of the 57 smolts tagged in Stewiacke River.

Many receivers were deployed in Minas Basin and Gaspereau River in 2019 and these have been used to study migration of alewives [24]. The same receivers and methods also enable examination of the migration of post-smolts that were tagged in Gaspereau River to the extent that this is relevant for the encounter problem. Of the 61 post-smolts detected beyond the mouth of Gaspereau River in 2019, all were detected by the receiver array at the mouth of Gaspereau River. Thus, the efficiency of that receiver array for detecting passing post-smolts was $\eta = 1$. A total of 71 smolts were detected by the receiver array

at the mouth of Gaspereau River, corresponding to 16 being lost within the Gaspereau River. Assuming no losses from the mouth of Gaspereau River to Minas Passage (i.e., as for 2022 measurements), then $N_{MP} = 71$ tagged post-smolts were expected to have reached Minas Passage.

In 2019, a total of 57 smolts were tagged and released in the Stewiacke River. The Stewiacke River runs into Shubenacadie River. Figure 1 shows 4 VR2W-180kHz receivers at the mouth of Shubenacadie River, which detected 26 smolts. A total of 33 post-smolts were detected by receivers in Minas Passage and Minas Basin at locations beyond the mouth of the Shubenacadie and 22 of those were also detected by receivers at the mouth of the Shubenacadie River. It follows that the receiver array at the mouth had detection efficiency $\eta = 22/33$ (67%) and given that a total of 26 smolts were detected passing the mouth it is expected that $26/\eta = 39$ smolts passed the mouth of Shubenacadie River. Thus, we expect that $57 - 39 = 18$ smolts were lost within the Stewiacke and Shubenacadie Rivers. As before, assuming no mortality in Minas Basin, as many as $N_{MP} = 39$ tagged post-smolts were expected to have reached Minas Passage.

3.2. Post-Smolt Motion in Minas Passage, Passing Events

In 2022, a HR2 receiver was suspended beneath a GPS-tracked drifter that moved with the currents through Minas Passage and neighbouring waters [9]. On three occasions, the HR2 detected signals from a tagged post-smolt that remained sufficiently close to the drifter to continue to be detected over 3–4 km track segments (red lines in Figure 4). Furthermore, the moored HR2 receivers detected the passing post-smolts at much later times when the drifter had moved by more than 10 km but was still relatively nearby the moored receiver when it detected the tagged post-smolt (Figure 4). Signals detected by receivers on and nearby the drifter demonstrate that post-smolts in Minas Passage are substantially displaced by/with the tidal currents/waters.

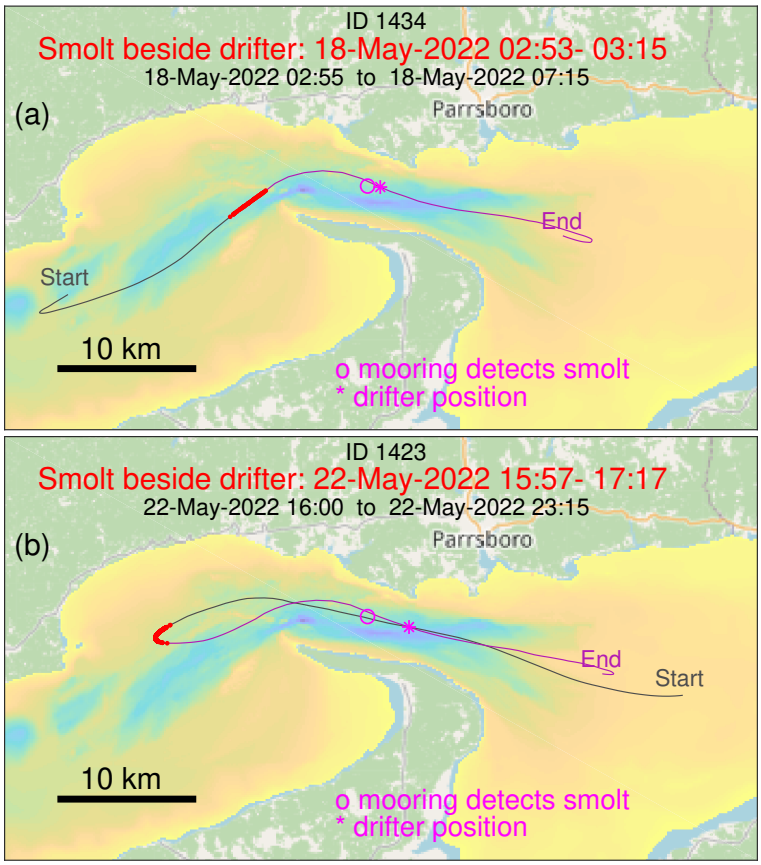

Figure 4. *Cont.*

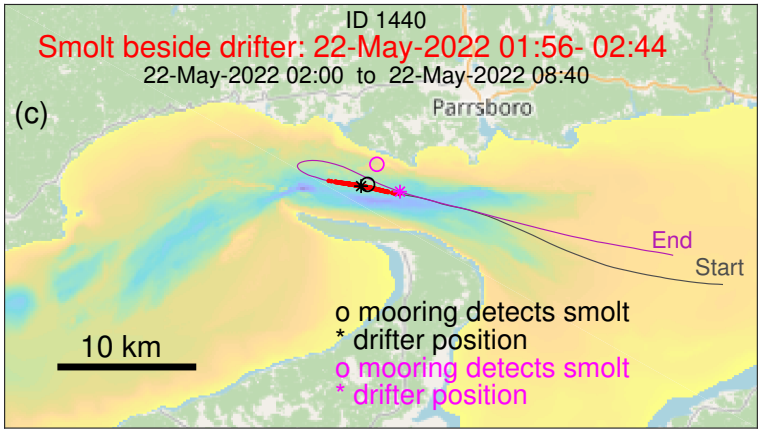

Figure 4. The black line shows a portion of the track of a drifter that has a HR2 receiver suspended beneath it. Red shows where the drifter was when its HR2 detected HR signals from a tagged post-smolt that was nearby. Subsequently, the tagged post-smolt was detected by a moored HR2 receiver (magenta circle) when the drifter was at a nearby position (magenta asterisk). (**a**) Detected on flood. (**b**) Detected low tide and flood. (**c**) Detected late ebb and early flood.

The duration of a passing event is defined as the time elapsed from first to the last HR signal detected during the passing event. Figure 5 shows the duration of each passing event measured by the FORCE line of 11 HR2 receivers that were deployed in 2022. It takes much less time for the tagged post-smolt to pass the receiver line when tidal current is fast. This is consistent with fast currents advecting post-smolts more quickly past receivers and reducing effective detection range [30].

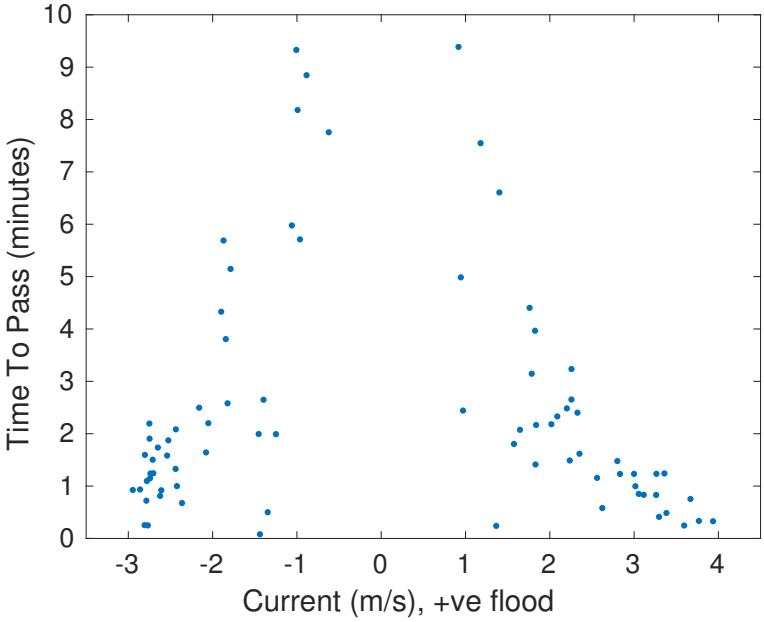

Figure 5. Duration of 2022 passing events diminishes with increasing current speed.

Given the fast tidal currents in Minas Passage, it is hardly surprising that post-smolts can be swept back and forth many times during their seaward migration. Figure 6 documents the number of passing events that the 2022 FORCE array measured for each smolt tagged in 2022. While two of the smolts never reached Minas Passage and another was only detected by the OTN line, other post-smolts were detected for up to eight passing events. Multiple passing events increases the likelihood of post-smolt-turbine interaction during migration, as has also been suggested for alewives [24] and striped bass [20].

The bars of Figure 6 are labelled with the days (elapsed since tagging) that span passing events recorded for each post-smolt. The time from tagging to first detected passing event ranged from 3 to 12 days (mean 8) and the time to last detected passing event ranged from 5 to 13 days (mean 10). The most passing events were measured for post-smolt 7, which had 8 passing events detected over a 6-day time span. Clearly, passing events were not detected on each flood-ebb tide, in part because the receiver array does not span the entire passage, but also because we should not think of post-smolts moving back and forth through Minas Passage with each successive ebb and flood tide because although some drifter trajectories exhibit such behaviour, others do not [9,10].

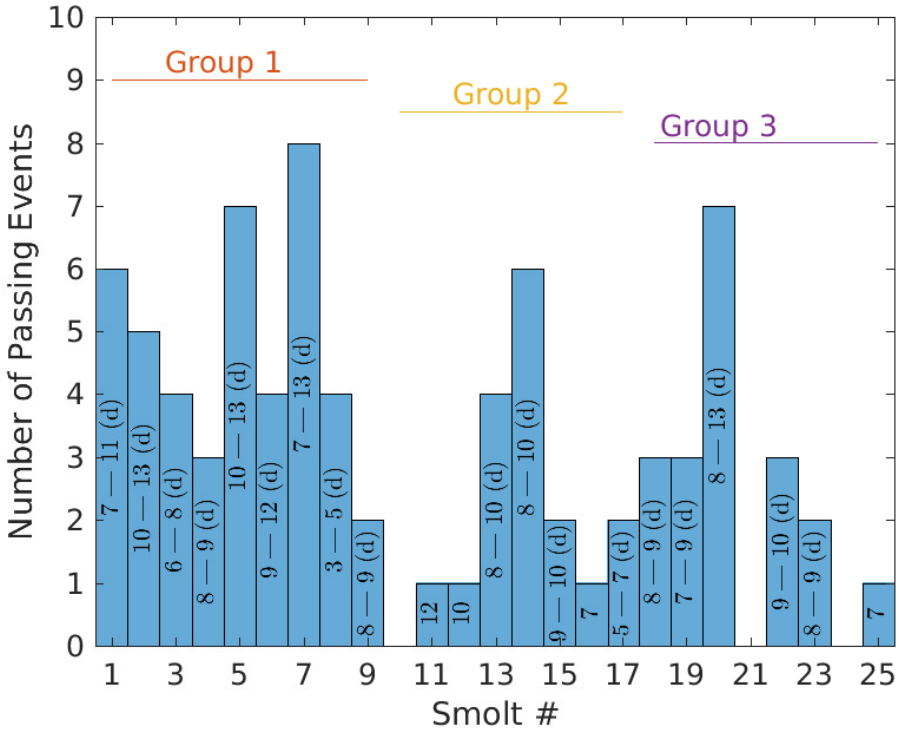

Figure 6. Post-smolts can cross the Minas Passage receiver array multiple times during their 2022 outbound migration.

3.3. Probabilities of Encounter for Post-Smolts in Minas Passage

Equation (9) obtains the half cross-current width scale λ for detection of a passing tag from p. Values for p have been obtained above from Eulerian measurements [30] of detection efficiency ρ and these give values for λ, as plotted by the blue circles in Figure 7. Values of λ rapidly diminish at large current speeds but $\lambda > W/2$ for all the current speeds for which λ was calculated. Values of p can be directly measured from tagged drifters that pass nearby a moored receivers (e.g., Figure 12 in [9]) and the red asterisks in Figure 7 show estimates of λ obtained from those measurements. Drifter measurements poorly resolved p with respect to range and current speed and the drifter tracks were mostly south of the TED area. Nevertheless, the two measurement methods show a broadly similar magnitude and trend for λ. Drifter measurements directly measure N_D as a function of the distance of the closest approach to the HR2 receiver (e.g., Figure 11 in [9]) and the fitted functions in that figure give the values of λ that are plotted with black dots in Figure 7. This final method seems to be the most straightforward way to obtain λ from drifter tracks.

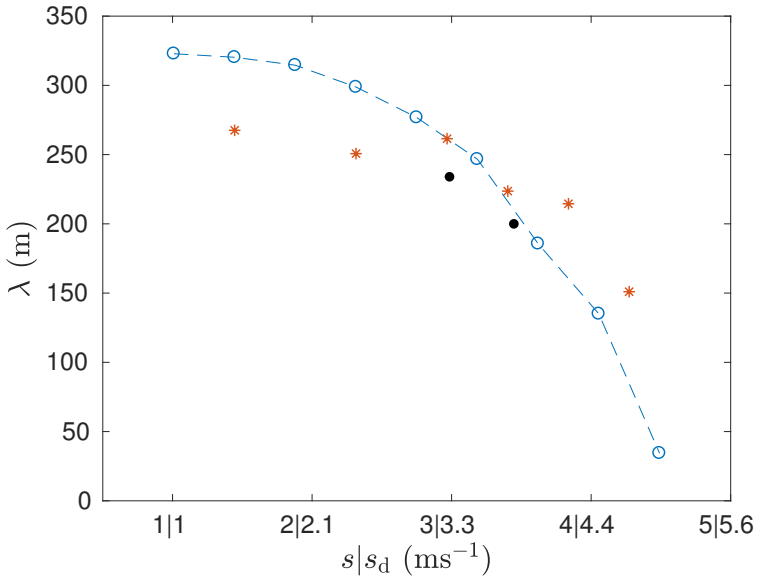

Figure 7. The half cross-current width scale for tag detection is a function of current speed. Blue circles show values obtained from Eulerian measurements of detection efficiency. Red asterisks show estimates obtained from Lagrangian measurements of p.

The trend for λ to decline with current speed (Figure 7) fundamentally defines the utility of our method for estimating the probability of encounter. As the current speed increases, the decline in λ shows that an individual HR2 receiver (proxy MHK turbine) will detect fewer tagged fish as they pass by, but λ appears in the denominator of (8), so this is offset by each detected passing event giving a higher value for $\mathcal{P}$. This compensating tendency will break down when λ becomes so small that limitations in the measurement of ρ also prevent λ from being numerically resolved. Figure 7 indicates that that limitation might start to apply for $s_d \approx 5$ ms^{-1}, but that is a somewhat tentative number because the calculation of λ then depends on values for ρ that are interpolated between measurements made at ranges of about 1 m and 40 m [9]. In addition, range tests must have a long duration to obtain a large sample size for such fast tidal currents.

A passing event $E_{n,j,k}$ is characterized by the identity number n of the post-smolt, the station number j of the HR2 that best detected the passing post-smolt, and the time k at which the post-smolt passed by. With respect to obtaining estimates of probability of encounter, the time and station number serve to obtain signed current speed s that applies to a passing event. Equation (8) can be used to calculate a probability of encounter $\mathcal{P}_{n,j,k}$ for each passing event, as illustrated in Table 1 for seven smolts tagged in 2022 and detected at stations j and times k when the drift current speed was s_d. Without a correction for correlated ρ fluctuations, the probabilities of encounter ${}^{E}\mathcal{P}_{n,j,k}$ (4) tend to be about 6% smaller than $\mathcal{P}_{n,j,k}$.

Table 1 lays out the sequence of passing events for individual post-smolts in 2022. It is notable that successive passing events of a mid-passage station ($j = 1$ or 2) were common, whereas successive passing events of a station in the TED area were rare. The one occasion when a post-smolt ($n = 5$) passed Station 12 on both a flood tide and the immediately following ebb tide was preceded by five passing events at mid-passage and other offshore sites. These observations of post-smolts are consistent with drifter tracks that have quasi-stable trajectories through mid-passage but not, apparently, through the TED area [10].

Table 1. Probability $\mathcal{P}$ that each passing event would result in an encounter with a turbine installation at the position of the receiver that detected the passing event. These results are for the passing events for post-smolts 1–7, which were tagged in Gaspereau River in 2022.

$\mathcal{P}_{n,j,k}$	${}^{E}\mathcal{P}_{n,j,k}$	$\mathbf{smolt}_n$	$\mathbf{stn}_j$	s_d (ms^{-1})	$\mathbf{time}_k$
0.0608	0.0595	1	1	−1.91	17-May 10:33
0.0597	0.0597	1	2	0.06	18-May 18:24
0.0649	0.0613	1	1	2.86	19-May 02:07
0.1333	0.1075	1	12	4.36	19-May 16:33
0.0755	0.0678	1	9	3.42	20-May 06:05
0.0727	0.0662	1	5	−3.71	20-May 09:36
0.0607	0.0595	2	1	−1.76	20-May 13:00
0.0799	0.0689	2	8	4.08	20-May 15:53
0.0691	0.0634	2	12	−3.19	21-May 11:08
0.0713	0.0652	2	4	−3.61	21-May 23:38
0.0614	0.0597	2	7	2.26	22-May 08:39
0.0597	0.0586	3	12	−1.75	16-May 09:12
0.0643	0.0599	3	4	−2.55	16-May 21:29
0.0747	0.0672	3	4	−3.84	17-May 07:09
0.0671	0.0624	3	6	3.09	17-May 16:42
0.0739	0.0669	4	1	−3.78	17-May 20:48
0.1140	0.0955	4	2	4.68	18-May 03:58
0.0872	0.0762	4	2	−4.13	18-May 08:54
0.0618	0.0601	5	6	2.32	20-May 07:09
0.0719	0.0665	5	2	3.53	20-May 19:12
0.0757	0.0678	5	2	−3.85	20-May 22:47
0.0817	0.0699	5	4	4.09	21-May 06:06
0.0650	0.0606	5	1	−2.85	21-May 12:43
0.0777	0.0680	5	12	3.52	22-May 05:10
0.0636	0.0596	5	12	−2.64	22-May 12:49
0.0608	0.0595	6	1	−1.88	19-May 12:09
0.0676	0.0621	6	10	−3.06	20-May 11:16
0.0695	0.0641	6	2	3.27	20-May 19:21
0.4116	0.2615	6	1	5.86	21-May 04:54
0.0603	0.0594	7	1	−1.37	16-May 22:28
0.0604	0.0595	7	1	1.73	16-May 23:56
0.0610	0.0595	7	1	−1.99	17-May 10:29
0.0591	0.0587	7	9	−0.92	19-May 00:08
0.0606	0.0596	7	2	1.76	19-May 01:32
0.0699	0.0651	7	9	3.09	20-May 15:40
0.0587	0.0585	7	11	0.73	21-May 20:46
0.0647	0.0603	7	7	−2.82	21-May 22:26

Presently, the probabilities of an encounter are not discounted for the possibility that a post-smolt might swim above or below the levels swept by the blades of a near-surface turbine installation. This adjustment is best left until such time as more engineering details are available for a specific MHK turbine installation. It is generally understood that post-smolts swim near the surface [28].

The n'th post-smolt makes K passing events with each passing event having some probability of encounter with a turbine installation at some station location j (Table 1). From those probabilities, we can calculate the expected number of times that the n'th post-smolt will encounter a turbine installation in the TED area during a time interval required for the tagged post-smolt to complete its seaward migration through Minas Passage. The expected number of times $\mathcal{E}_{n,\mathrm{TED}}$ that post-smolt n will encounter a single turbine installation within the TED area can be estimated using

$$\mathcal{E}_{n,\mathrm{TED}} = \frac{1}{4}\sum_{k=1}^{K}\mathcal{P}_{n,9\leq j\leq 12,k} \tag{10}$$

where the sum term is over those K passing events of four HR2 receivers within the TED area ($9 \leq j \leq 12$). Thus, the factor of $1/4$ normalizes to the expected number of times that post-smolt n would encounter a single turbine installation within the TED area. Although (10) is written to calculate $\mathcal{E}_{n,\mathrm{TED}}$ from $\mathcal{P}_{n,j,k}$, it equally applies to calculate ${}^{E}\mathcal{E}_{n,\mathrm{TED}}$ from values of ${}^{E}\mathcal{P}_{n,j,k}$. Similarly, selecting stations $1 \leq j \leq 2$ and normalizing by $1/2$ gives a mid-passage value $\mathcal{E}_{n,\mathrm{mid-passage}}$.

Averaging over all 23 post-smolts that reached Minas Passage in 2022 gives an estimate for the average number of times $\overline{\mathcal{E}}_{\mathrm{TED}}$ that a post-smolt might be expected to encounter a single turbine installation within the TED area

$$\overline{\mathcal{E}}_{\mathrm{TED}} = \frac{1}{23} \sum_{n=1}^{23} \mathcal{E}_{n,\mathrm{TED}}. \tag{11}$$

Figure 8 shows $\mathcal{E}_{n,\mathrm{TED}}$ for each tagged post-smolt that was estimated to have reached Minas Passage in the years 2019 and 2022. Note, for easy visualization we have renumbered the post-smolts in order of descending values of $\mathcal{E}_{n,\mathrm{TED}}$. There are many zero values for $\mathcal{E}_{n,\mathrm{TED}}$ because, of the N_{MP} post-smolts that were estimated to reach Minas Passage, only N_{TED} passed through the TED area (Table 2). Of those post-smolts that were detected within the TED area ($\mathcal{E}_{n,\mathrm{TED}} > 0$), values for $\mathcal{E}_n$ tended to be highest for 2019 post-smolts that were tagged in the Stewiacke River and lowest for 2022 post-smolts that were tagged in the Gaspereau River. High values of $\mathcal{E}_n$ for the post-smolts tagged in the Stewiacke River are, at least in part, associated with a relatively large ratio of the number E_{TED} of passing events that they make through the TED area relative to the number N_{TED} of post-smolts that passed through the TED area (Table 2).

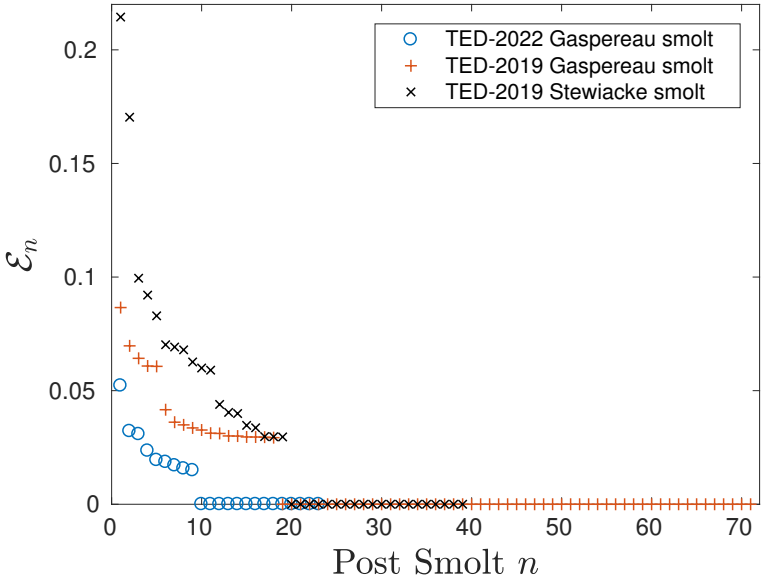

Figure 8. Expected number of encounters that each post-smolt would make with a single turbine installation at the TED area.

Table 2 indicates no meaningful difference between the 2019 and 2022 measurements of the average number of encounters $\overline{\mathcal{E}}_{\mathrm{TED}}$ for post-smolts that came from the Gaspereau River. On the other hand, $\overline{\mathcal{E}}_{\mathrm{TED}}$ is substantially greater for 2019 post-smolts from the Stewiacke River. These values are sensitive to the ratio of E_{TED} to N_{MP}. In 2022, the value of N_{MP} was confirmed in two ways. First, from measurements of tagged smolts travelling through the Gaspereau River, and second, by the extensive arrays (OTN and FORCE) of HR2 receivers in Minas Passage. In 2019, there were relatively few HR2 receivers deployed in Minas Passage, so estimates of the number of tagged post-smolts reaching Minas Passage N_{MP} are more open to question.

Table 2. Relating the expected number of encounters to the number of post-smolts detected in Minas Passage N_{MP} and at the TED area N_{TED}.

Post Smolts	N_{MP}	N_{TED}	E_{TED}	$\overline{\mathcal{E}}_{TED}(\mathcal{E}_{n,TED} > 0)$	$\overline{\mathcal{E}}_{TED}$
2022 Gaspereau	23	9	11	0.025 ± 0.004	0.010 ± 0.003
2019 Gaspereau	71	18	22	0.042 ± 0.004	0.011 ± 0.002
2019 Stewiacke	39	19	38	0.070 ± 0.011	0.034 ± 0.008

The 29 Stewiacke post-smolts that FORCE Minas Passage receivers detected in 2019 averaged 7.8 passing events each. This was considerably higher than the average of 3.0 passing events for the 43 Gaspereau post-smolts that were detected by the same receivers in Minas Passage. Taking values of N_{MP} at face value, Table 2 indicates that post-smolts from the Stewiacke River were more likely to migrate through the northern side of Minas Passage (i.e., through the TED area) than post-smolts from the Gaspereau River. This apparent difference is based on measurements made in a single year, so the result is tentative. Nevertheless, there might be a physical explanation for this difference. There is evidence for a clockwise gyre in the southern arm of Minas Basin [32,33]. Smolts migrating from Gaspereau River might be transported by this gyre, which would tend to put them on trajectories that would be more likely to pass through the mid or southern half of Minas Passage.

It might be argued that post-smolt encounters with turbines are benign at a sufficiently small current speed. Discarding $\mathcal{P}_{n,j,k}(|s_d| < 1)$ leaves an expected number of encounters applicable to an assumption that harm can only result if $|s_d| \geq 1$ m/s. Successive rows in Table 3 show how the number of harmful encounters drops as the threshold current is increased. The threshold current for harm is expected to depend upon the specific design of the turbines. For example, in order to approach the Betz limit the turbine blades typically have a tip speed much greater than the current speed [34] and harm becomes more likely for strike speeds above 5 m/s [35].

Table 3. Expected number of times that a smolt would encounter a single turbine installation during its seaward migration from the Gaspereau and Stewiacke Rivers.

2022 Gaspereau River		2019 Gaspereau River		2019 Stewiacke River		$\lvert s_d \rvert$
$\overline{\mathcal{E}}_{TED}$	$\overline{\mathcal{E}}_{mid-passage}$	$\overline{\mathcal{E}}_{TED}$	$\overline{\mathcal{E}}_{S2}$	$\overline{\mathcal{E}}_{TED}$	$\overline{\mathcal{E}}_{S2}$	(ms^{-1})
0.0098 ± 0.0030	0.075 ± 0.031	0.0110 ± 0.0024	0.014 ± 0.004	0.034 ± 0.0078	0.075 ± 0.017	≥ 0
0.0091 ± 0.0028	0.073 ± 0.031	0.0087 ± 0.0022	0.014 ± 0.004	0.032 ± 0.0078	0.072 ± 0.017	≥ 1
0.0091 ± 0.0028	0.072 ± 0.031	0.0082 ± 0.0022	0.013 ± 0.004	0.03 ± 0.0079	0.063 ± 0.016	≥ 1.5
0.0085 ± 0.0029	0.069 ± 0.032	0.0074 ± 0.0021	0.011 ± 0.004	0.026 ± 0.0071	0.058 ± 0.015	≥ 2
0.0078 ± 0.0029	0.067 ± 0.031	0.0070 ± 0.0020	0.008 ± 0.004	0.024 ± 0.0064	0.044 ± 0.013	≥ 2.5

Table 3 also compares the expected number of encounters with a turbine installation within the TED area (Figure 2) with an installation near mid-passage (Station 1 or 2 in 2022 and Station S2 in 2019). The number of encounters is greater for a turbine installation near the middle of Minas Passage than within the TED area. This is consistent with previous qualitative observations of tagged striped bass being detected more frequently to the south of the TED area than within the TED area [20]. There are two physical mechanisms that might be related to this result. First, the water column having been more stretched in the vertical (more horizontal convergence) as it passed into those deeper waters to the south of the TED area [36]. Such a convergence would concentrate animals that maintain their vertical component of position near the sea surface. Second, there is a quasi-stable drifter trajectory through mid-passage [10] so that post-smolts that get on that trajectory might pass many times back and forth with the tide.

4. Discussion

Fish mortality caused by a low-head turbine can sometimes be estimated by recovering all fish after they passed through the turbine [5,6]. It seems improbable that such straightforward and comprehensive methodology could be adapted to obtain mortality caused by a MHK turbine in the TED area in Minas Passage. A harm reduction premise of a MHK turbine is to enable free passage around the turbine, which makes recovering all fish that pass through the turbine an ill-defined objective unless their detailed trajectories are first accurately determined.

It seems more feasible to break the fish-turbine interaction problem into sequential parts, at least some of which may be tractable for measurement. First, identify whether local populations of interest are found at a TED area [20,21,24], in which case they might be said to have *co-occurrence* with MHK turbines. Estimation of the probability of encounter $\mathcal{P}$ might be considered a next step towards estimating percentage harm or mortality for a population.

We have defined the probability of encounter and calculated and measured it in a way that is consistent with modelling a local population. Elsewhere [15,37], metrics that were called "probability of encounter" are different in kind from those that we have defined and calculated. The metrics obtained by [15,37] are of interest in their own right but they cannot be compared to what we have carried out.

The present calculations of the probability of encounter are based upon a 500 kW near-surface installation of 6 MHK turbines set side-by-side in the FORCE TED area [10,25,26]. It is generally understood that post-smolts swim near the surface [28] so the probability of encounter takes no account of the possibility that some fish might swim at levels different from those swept by the turbine blades. Some measurements of post-smolt swimming depth have been made in Minas Passage [27] but it is presently unclear whether these will be sufficient for a robust calculation of the overlap of swimming depth with some specific turbine installation. More measurements of post-smolt swimming depth may be required. Swimming depth can be a key factor for the probability of encounter in the TED area, so a near-surface turbine is expected to have little overlap with striped bass [20] and a near-seafloor turbine to have little overlap with post-smolts.

A given post-smolt may pass through the TED area more than once during its seaward migration so we have summed over probabilities of encounter and normalized in order to estimate an average number of encounters $\overline{\mathcal{E}}_{\mathrm{TED}}$ that a post-smolt would be expected to make with a turbine installation within the TED area. If every encounter was fatal at current speeds greater than 1 ms^{-1}, then that single turbine installation would cause approximately a 0.9% loss in the out-migrating population of post-smolts from the Gaspereau River and about a 3% loss of post-smolts from the Stewiacke River. Loses during the downriver migration were much higher (32% for the Stewiacke River in 2019, 18% for the Gaspereau River in 2019, and 8% for the Gaspereau River in 2022), although some of those losses may be a result of tagging effects and large downriver losses should not be thought to be inevitable [38]. It has been estimated that the average at-sea mortality of immature salmon was 97% for the 1990–2003 time period [29], so 0.9% or 3% out-migration losses caused by turbine installation would only add 0.027% or 0.09% to the 97% at-sea mortality. On the other hand, at-sea losses of immature salmon have not always been so high [29] and if the causes for those losses were identified and corrected then encounters of post-smolts with the turbine installation may be deemed more problematic. In this sense, the management of MHK turbine installations is fundamentally entangled with the management of fish populations in general.

Measuring the expected number of encounters $\overline{\mathcal{E}}_{\mathrm{TED}}$ requires an accurate estimate of the number N_{MP} of tagged post-smolts that reach Minas Passage. The 2022 array of HR2 receivers reliably detected tags passing through the central and northern portion of Minas Passage but did not extend sufficiently to the south to monitor all passing events [9]. Nevertheless, the 2022 array was sufficient to accurately determine N_{MP} because most post-smolts make multiple passes through the passage so the odds were improved that

at least one pass was through that part of the passage that was monitored. Larger fish may move more independently of the tidal currents and so it would be desirable for the receiver array to extend all the way across Minas Passage. The limited extent of the 2019 array makes corresponding estimates of N_{MP} less certain. A relatively large value of $\overline{\mathcal{E}}_{TED}$ must still stand for the post-smolts that were tagged in the Stewiacke River because the largest possible value for N_{MP} would be 57, which is only sufficient to diminish $\overline{\mathcal{E}}_{TED}$ from 0.032 to 0.022. On the other hand, the 2019 post-smolts from the Gaspereau River had a logically smallest value for N_{MP} of 43 (the number detected in Minas Passage), which would increase $\overline{\mathcal{E}}_{TED}$ to 0.014. It is unlikely that both extremes of N_{MP} would apply, so it seems that in 2019 $\overline{\mathcal{E}}_{TED}$ was larger for post-smolts from the Stewiacke River than for those from the the Gaspereau River. The proximate reason is that 2019 Stewiacke post-smolts made more passes through the TED area. More fundamentally this might indicate some difference in post-smolt trajectories to Minas Passage depending upon whether they began at the mouth of the Schubenacadie River or the mouth of the Gaspereau River. Further work is required to elucidate whether such differences are repeated and, if so, why?

The tip speed of a MHK turbine blade must be much faster than the current speed in order for the turbine to efficiently extract tidal energy [11,34]. Nevertheless, the current speed at which turbine blades become dangerous is unknown for specific turbines and operational procedures that might apply for future installations in Minas Passage. $\overline{\mathcal{E}}_{TED}$ was, therefore, estimated for a range of critical current speeds, s_d from 0 to 2.5 ms^{-1}. $\overline{\mathcal{E}}_{TED}$ typically declined by about 30% over that current range (Table 3).

Probability of encounter was estimated using a method that does not actually have a turbine installation in place. This was performed deliberately because where a turbine is installed it might influence fish behaviour, either by causing them to aggregate at the installation near slack tide [13,18] or to avoid the installation during fast currents [15–18]. A turbine operating near the Betz limit [11] will divert approximately one third of the approaching flow around the turbine, so if fish simply follow the flow then it should be expected that one third of them will avoid the turbine. Flume tank studies [14] showed salmon passing above the downwards sweeping blade, consistent with following deflected flow. It is expected that near surface MHK turbines that operate near the Betz limit would generate vibrational energy which fish might detect and respond to, perhaps by avoiding the area swept by turbine blades. This possibility has not been measured within the TED area in Minas Passage.

Presently, we have calculated the probability of encounter $\mathcal{P}$ from an ensemble averaged estimate of detection efficiency $\rho(r, s)$ with a small empirical correction (5) for fluctuations about the typical value at a given range r and modelled current speed s. In principle, signal detection is more fundamentally related to ambient noise level than modelled current or some other environmental variable. This raises the prospect of more directly estimating detection efficiency by directly measuring ambient levels at the 170 kHz frequency of HR signals and, perhaps, obtaining estimates of probability of encounter that are more specific to time and place.

The calculation of λ becomes uncertain in very fast currents (Figure 7) because very few measurements of ρ were obtained when $s > 4$ ms^{-1} [30]. Targeted range-test experiments to augment existing values for ρ should be carried out in the TED area during the largest spring tides with separations of tags and receivers to resolve ranges <50 m. Better mooring technology should be used to keep HR2 receivers sufficiently clear of the seafloor so signal paths are not blocked [30]. Based upon the present work, we recommend using tagged drifters to better quantify how well ρ relates to the detection of tagged fish as they pass the HR2 array [9]. Tagged drifters should also be used to obtain independent estimates of p and λ [9], and thereby enable independent spot checks of p and λ obtained from ρ. In the difficult field conditions encountered in Minas Passage, it is important to have multiple lines of evidence that confirm results.

In conclusion, we have measured the probabilities that post-smolts would encounter a turbine installation in the TED area in Minas Passage and have provided some context

for interpreting those probabilities. The probability that post-smolts will be harmed is expected to be lower than their probability of encounter because some might avoid the turbine or not suffer harm even though they pass through the area swept by turbine blades. It is hoped that the work will be useful for guiding future studies and, in the interim, be useful for assessing the merit of installing MHK turbines in the TED area relative to the ecological harm that they might inadvertently cause.

Author Contributions: Conceptualization, B.G.S. and D.J.H.; methodology, B.G.S., R.H.K. and D.J.H.; validation, B.G.S., D.J.H. and R.H.K.; formal analysis, B.G.S.; investigation, B.G.S., C.C.S., D.J.H. and D.C.H.; writing—original draft preparation, B.G.S.; writing—review and editing, B.G.S., R.H.K., D.J.H., D.C.H. and C.C.S.; visualization, B.G.S.; supervision, B.G.S. and D.J.H.; project administration, D.J.H. and B.G.S.; funding acquisition, D.J.H., D.C.H. and B.G.S. All authors have read and agreed to the published version of the manuscript.

Funding: This research was funded by Natural Resources Canada, grant number ERPP-RA-07.

Institutional Review Board Statement: The animal study protocol was approved by the Animal Care Committee of Acadia University (#07-18 and #08-22).

Informed Consent Statement: Not applicable

Data Availability Statement: Datasets analyzed during the present study are available from the corresponding author upon reasonable request.

Acknowledgments: Acadia Centre for Estuarine Research helped fund drifter experiments and provided laboratory space and equipment. Randy Corcoran assisted with the deployment and recovery of drifters. Minas Passage moorings were deployed and recovered by Shaun Allain with the assistance of Mike Huntley and the crew of the Nova Endeavour. The Ocean Tracking Network provided measurements from the receiver array that they maintain in Minas Passage.

Conflicts of Interest: The authors declare no conflict of interest. The funders had no role in the design of the study; in the collection, analyses, or interpretation of data; in the writing of the manuscript; or in the decision to publish the results.

Abbreviations

The following abbreviations are used in this manuscript:

FORCE	Fundy Ocean Research Centre for Energy
DFO	Department of Fisheries and Oceans, Canada
OTN	Ocean Tracking Network, Canada
MHK	Marine hydrokinetic
TED	Tidal Energy Demonstration
PPM	Pulse position modulation
HR	High residency
HR2	High residence receiver
FVCOM	Finite-Volume Coastal Ocean Model
GPS	Global Positioning System

References

1. Price, D. Energy and human evolution. *Popul. Environ.* **1995**, *16*, 301–319. [CrossRef]
2. May, R.M. Ecological science and tomorrow's world. *Philosphical Trans. R. Soc. B* **2010**, *365*, 41–47. [CrossRef] [PubMed]
3. Karsten, R.; McMillan, J.; Lickley, M.; Haynes, R. Assessment of tidal current energy in the Minas Passage, Bay of Fundy. *J. Power Energy* **2008**, *222*, 289–297. [CrossRef]
4. Lenders, H.J.R.; Chamuleau, T.P.M.; Hendriks, A.J.; Lauwerier, R.C.G.M.; Leuven, R.S.E.W.; Verberk, W.C.E.P. Historical rise of waterpower initiated the collapse of salmon stocks. *Sci. Rep.* **2016**, *6*, 29269. [CrossRef] [PubMed]
5. DuBois, R.B.; Gloss, S.P. Mortality of juvenile shad and striped bass passed through Ossberger crossflow turbines at a small-scale hydroelectric site. *N. Am. J. Fish. Manag.* **1993**, *13*, 178–185. [CrossRef]
6. Watson, S.M.; Schneider, A.D.; Gardner, L.C.; Apell, B.R.; Thompson, P.C.; Cadman, G.B.; Gagnon, I.F.; Frese, C.R.; Wechsler, J.F. Juvenile alewife passage through a compact hydropower turbine designed for fish safety. *N. Am. J. Fish. Manag.* **2023** , *43*, 465–475. [CrossRef]

7. Dadswell, M.J.; Rulifson, R.A. Macrotidal estuaries: A region of collision between migratory marine animals and tidal power development. *Biol. J. Linn. Soc.* **1994**, *51*, 93–113. [CrossRef]
8. Karsten, R. An assessment of the potential of tidal power from Minas Passage, Bay of Fundy, using three-dimensional models. In Proceedings of the ASME 2001 30th International Conference on Ocean, Offshore and Arctic Engineering, OMEA2011-49249, Rotterdam, The Netherlands, 19–24 June 2011.
9. Sanderson, B.G.; Karsten, R.; Hasselman, D.J. Using drifters equipped with acoustic tags to verify the utility of detection efficiency measurements for estimating probability of fish-turbine encounter. *J. Mar. Sci. Eng.* 2023, *submitted*.
10. Sanderson, B.G.; Stokesbury, M.J.W.; Redden, A.M. 2021. Using trajectories through a tidal energy development site in the Bay of Fundy to study interaction of renewable energy with local fish. *J. Ocean. Technol.* **2021**, *16*, 50–70.
11. Betz, A. *Introduction to the Theory of Flow Machines*; Randall, D.G., Translator; Pergamon Press: Oxford, UK, 1966.
12. Hammar, L.; Andersson, S.; Eggertsen, L.; Haglund, J.; Gullstrom, M.; Ehnberg, J.; Molander, S. Hydrokinetic Turbine Effects on Fish Swimming Behaviour. *PLoS ONE* **2013**, *8*, e84141. [CrossRef]
13. Broadhurst, M.; Barr, S.; Orme, D. In-Situ Ecological Interactions with a Deployed Tidal Energy Device; An Observational Pilot Study. *Ocean. Coast. Manag.* **2014**, *99*, 31–38. [CrossRef]
14. Castro-Santos, T.; Haro, A. Survival and behavioral effects of exposure to a hydrokinetic turbine on juvenile Atlantic salmon and adult American Shad. *Estuaries Coasts* **2015**, *38* (Suppl. S1), 203–214. [CrossRef]
15. Shen, H.; Zydlewski, G.; Viehman, H.; Staines, G. Estimating the probability of fish encountering a marine hydrokinetic device. *Renew. Energy* **2016**, *97*, 746–756. [CrossRef]
16. Grippo, M.; Zydlewski, G.; Shen, H.; Goodwin, R.A. Behavioral responses of fish to a current-based hydrokinetic turbine under mutliple operational conditions. *Environ. Monit. Assess.* **2020**, *192*, 645. [CrossRef]
17. Viehman, H.A.; Zydlewski, G.B. Fish Interactions with a Commercial-Scale Tidal Energy Device in the Natural Environment. *Estuaries Coasts* **2015**, *38* (Suppl S1), S241–S252. [CrossRef]
18. Fraser, S.; Williamson, B.J.; Nikora, V.; Scott, B.E. Fish distributions in a tidal channel indicate the behavioural impact of a marine renewable energy installation. *Energy Rep.* **2018**, *4*, 65–69. [CrossRef]
19. Viehman, H.A.; Hasselman, D.J.; Douglas, J.; Boucher, T. The ups and downs of using active acoustic technologies to study fish at tidal energy sites. *Front. Mar. Sci.* **2022**, *9* , 1–16. [CrossRef]
20. Keyser, F.; Redden, A.M.; Sanderson, B.G. Winter presence and temperature-related diel vertical migration of Striped Bass *Morone saxatilis* in an extreme high flow passage in the inner Bay of Fundy. *Can. J. Fish. Aquat. Sci.* **2016**, *73*, 1777–1786. [CrossRef]
21. Stokesbury, M.J.W.; Logan-Chesney, L.M.; McLean, M.F.; Buhariwalla, F.F.; Redden, A.M.; Beardsall, J.W.; Broome, J.; Dadswell, M.J. Atlantic sturgeon spatial and temporal distribution in Minas Passage, Nova Scotia: A region of future tidal power extraction. *PLoS ONE* **2016**, *11*, e0158387. [CrossRef]
22. Lilly, J.; Dadswell, M.J.; McLean, M.f.; Avery, T.S.; Comolli, P.D.; Stokesbury, M.J.W. Atlantic sturgeon presence in a designated marine hydrokinetic test site prior to turbine deployment: A baseline study. *J. Appl. Ichthyol.* **2021**, *37*, 826–834. [CrossRef]
23. Sanderson, B.G.; Buhariwalla, C.; Adams, M.; Broome, J.; Stokesbury, M.; Redden, A.M. Quantifying detection range of acoustic tags for probability of fish encountering MHK devices. In Proceedings of the 12th European Wave and Tidal Energy Conference, Cork, Ireland, 27 August–1 September 2017.
24. Tsitrin, E.; Sanderson, B.G.; McLean, M.F.; Gibson, A.J.F.; Hardie, D.C.; Stokesbury, M.J.W. Migration and apparent survival of postspawning alewife (Alosa pseudoharengus) in Minas Basin, Bay of Fundy. *Anim. Biotelemetry* **2022**, *10*, 11. [CrossRef]
25. Davie, E. Tidal Energy Companies Join Forces for Bay of Fundy Project. CBC News. 2019. Available online: www.cbc.ca/news/canada/nova-scotia/sustainable-marine-energy-minas-tidal-lp-bay-of-fundy-tidal-power-1.5304276 (accessed on 1 March 2023).
26. Jeffcoate, P.; McDowell, J. Performance of PLAT-I, a floating tidal energy platform for inshore applications. In Proceedings of the 12th European Wave and Tidal Energy Conference, Cork, Ireland, 27 August–1 September 2017.
27. Solda, C. Migration Ecology of Inner Bay of Fundy Atlantic Salmon (*Salmo Salar*) Smolt, and the Relationship between Improvements in Tagging Technology and Surgical Procedures and Estimates of Post Surgery Survival. Master's Thesis, Acadia University, Wolfville, NS, Canada, 2023. *in preparation*.
28. Renkawitz, M.D.; Sheehan, T.F.; Goulette, G.S. Swimming depth, behavior, and survival of Atlantic salmon postsmolts in Penobscot Bay, Maine. *Trans. Am. Fish. Soc.* **2012**, *141*, 1219–1229. [CrossRef]
29. DFO. Recovery Potential Assessment for Inner Bay of Fundy Atlantic Salmon. DFO Canadian Science Advisory Secretariat Science Advisory Report 2008/050. 2008. Available online: https://waves-vagues.dfo-mpo.gc.ca/library-bibliotheque/335147.pdf (accessed on 1 March 2023).
30. Sanderson, B.G.; Bangley, C.W.; McGarry, L.P.; Hasselman, D.J. Measuring detection efficiency of 170 kHz high-residency acoustic signals in a fast-flowing tidal passage. *J. Mar. Sci. Eng.* 2023, *submitted*.
31. Chen, C.; Beardsley, R.C.; Cowles, G. An unstructured-grid, finite-volume coastal ocean model (FVCOM) system. *Oceanography* **2006**, *19*, 78–89. [CrossRef]
32. Greenberg, D.A. Modelling the mean barotropic circulation in the Bay of Fundy and Gulf of Maine. *J. Phys. Oceanogr.* **1983**, *13*, 886–904. [CrossRef]
33. Tee, K.T. Tide induced residual motion—verification of a numerical model. *J. Phys. Oceanogr.* **1977**, *7*, 396–402. [CrossRef]
34. Bahaj, A.S. Marine current energy conversion: The dawn of a new era in electricity production. *Phil. Trans. R. Soc. A* **2013**, *317*, 20120500. [CrossRef]

35. Amaral, S.V.; Bevelhimer, M.S.; Cada, G.F.; Giza, D.J.; Jacobson, P.T.; McMahon, B.J.; Pracheil, B.M. Evaluation of Behavior and Survival of Fish Exposed to an Axial-Flow Hydrokinetic Turbine. *N. Am. J. Fish. Manag.* **2015**, *35*, 97–113. [CrossRef]
36. Okubo, A. Horizontal dispersion of floatable particles in the vicinity of velocity singularities such as convergences. *Deep.-Sea Res.* **1970**, *17*, 445–454. [CrossRef]
37. Viehman, H.; Boucher, T.; Redden, A.M. Winter and summer differences in probability of fish encounter (spatial overlap) with MHK devices. In Proceedings of the 12th European Wave and Tidal Energy Conference, Cork, Ireland, 27 August–1 September 2017.
38. Newton, M.; Barry, J.; Dodd, J.A.; Lucas, M.C.; Boylan, P.; Adams, C.E. A test of the cumulative effect of river weirs on downstream migration success, speed and mortality of Atlantic salmon (*Salmo salar*) smolts: An empirical study. *Ecol. Freshwat. Fish* **2018**, *28*, 176–186. [CrossRef]